

Band nesting and the optical response of two-dimensional semiconducting transition metal dichalcogenides

A. Carvalho¹, R. M. Ribeiro^{1,2}, A. H. Castro Neto¹

¹Graphene Research Centre, National University of Singapore, 6 Science Drive 2, Singapore 117546 and

²Center of Physics and Department of Physics, University of Minho, PT-4710-057, Braga, Portugal

(Dated: November 1, 2018)

We have studied the optical conductivity of two-dimensional (2D) semiconducting transition metal dichalcogenides (STMDC) using *ab initio* density functional theory (DFT). We find that this class of materials presents large optical response due to the phenomenon of *band nesting*. The tendency towards *band nesting* is enhanced by the presence of van Hove singularities in the band structure of these materials. Given that 2D crystals are atomically thin and naturally transparent, our results show that it is possible to have strong photon-electron interactions even in 2D.

PACS numbers: 71.20.Mq,78.40.Fy,71.10.-w

STMDC is a family of 2D crystals with a chemical formula MX_2 where $M = W, Mo, Ti, Zr, Hf, Pd, Pt$, and others, and $X = S, Se, Te$,¹⁻³ whose crystals are formed by one layer of transition metal atoms sandwiched by other two layers of chalcogens, all triangular lattices, in either trigonal prismatic (T) or octahedral (O) geometry. Most of them have band gaps in the visible range, between 1 eV and 3 eV, and have been the subject of study in the last few years^{4,5} since the emergence of the field of 2D crystals.⁶ Because of these band gaps, in a technologically interesting range, these materials are being considered for a new generation of 2D transistor, sensor, and photovoltaic applications.

It was discovered recently⁷ that these materials have strong optical properties even when they are only three atoms thin. This is rather surprising because atomically thin films like these, only tens of Angstroms in thickness, are naturally transparent and we would not expect a strong photon-electron coupling *a priori*. In this letter, we show that this extraordinary optical response is due to the phenomenon of *band nesting*, namely, the fact that in the band structure of these materials there are regions where the conduction and valence bands are parallel to each other in energy. Band nesting implies that when the material absorbs a photon, the produced electrons and holes propagate with exactly the same, but opposite, velocities. Thus, the center of mass motion of the electron-hole pair is frozen. We find that band nesting is present in the band structure of all these materials. Furthermore, the existence of strong van Hove singularities (VHS) facilitates the phenomenon of band nesting.

In semiconductors, the band gap plays an important role in what concerns optical absorption. It defines the threshold after which there is absorption of electromagnetic radiation, by the promotion of an electron from the valence band to the conduction band. But the largest absorption is usually not at the band gap edge; it is often considered to be in a VHS in the electronic structure. These correspond to singularities in the density of states; if it happens both in the conduction and the valence band, there will be a strong photon absorption. Yet, this coincidence can only happen in a high symme-

try point, and there are very few in the Brillouin Zone (BZ). A particular case is the extended van Hove singularity (EVHS) in that these are single band saddle points with a flat band in one of the directions.⁸

The optical conductivity of a material can be written as:

$$\sigma_1(\omega) = \kappa_2(\omega)\omega\epsilon_0,$$

where $\kappa_2(\omega)$ is the imaginary part of the relative electric permittivity, ω is the frequency of the incoming electromagnetic radiation, and ϵ_0 is the vacuum permittivity. In the optical dipole approximation we can write:

$$\kappa_2(\omega) = A(\omega) \sum_{v,c} \int_{BZ} \frac{d^2\mathbf{k}}{(2\pi)^2} |d_{vc}|^2 \delta(E_c - E_v - \hbar\omega), \quad (1)$$

where the sum is over the occupied states in the valence band (v) and the unoccupied states in the conduction band (c), and includes implicitly the sum over spins, $A(\omega) = 4\pi^2 e^2 / (m^2 \omega^2)$ (e is the electric charge and m the carrier mass), d_{vc} is the dipole matrix element. The integral in (1) is evaluated over the entire 2D BZ. If we consider cuts $S(E)$ of constant energy E , $E = \hbar\omega = E_c - E_v$, in the band structure, we can write:

$$d^2\mathbf{k} = dS \frac{d(E_c - E_v)}{|\nabla_k(E_c - E_v)|},$$

and the integral in (1) can be rewritten as:

$$\kappa_2(\omega) = A(\omega) \sum_{v,c} \frac{1}{(2\pi)^2} \int_{S(\omega)} \frac{dS}{|\nabla_k(E_c - E_v)|} |d_{vc}|^2.$$

Notice that the strong peaks in the optical conductivity will come from regions in the spectrum where $|\nabla_k(E_c - E_v)| \approx 0$. If d_{vc} varies slowly over these regions (so that there is a gradient expansion) we can write:

$$\kappa_2(\omega) \approx A(\omega) \sum_{v,c} |d_{vc}|^2 \rho_{vc}(\omega),$$

where

$$\rho_{vc}(\omega) = \frac{1}{(2\pi)^2} \int_{S(\omega)} \frac{dS}{|\nabla_k(E_c - E_v)|},$$

is the joint density of states (JDOS).

The points where $\nabla_k (E_c - E_v) = 0$ are called critical points (CP) and they can be of several types. If $\nabla_k E_c = \nabla_k E_v = 0$ we have either a maximum, a minimum or a saddle point in each band; this can occur only in high symmetry points. Usually, these points receive more attention, because they are easy to pinpoint by visual inspection of the band structure, and give rise to peaks in the DOS. On the other hand, the condition $\nabla_k (E_c - E_v) = 0$ with $|\nabla_k E_c| \approx |\nabla_k E_v| > 0$, that is *band nesting*, can be satisfied in any part of the BZ but they are not immediately identified by eyeballing. Notice that this condition differs from an EVHS⁸ in that the later refers to saddle points in one band, while the proposed band nesting is determined by the “topographic” difference between the conduction and valence bands.

We performed a series of DFT calculations for the STMDC family using the open source code QUANTUM ESPRESSO⁹. We used norm conserving, full relativistic pseudopotentials with nonlinear core-correction and spin-orbit information to describe the ion cores.¹⁰ The exchange correlation energy was described by the generalized gradient approximation (GGA), in the scheme proposed by Perdew-Burke-Ernzerhof¹¹ (PBE). The Brillouin-zone (BZ) was sampled for integrations according to the scheme proposed by Monkhorst-Pack^{12,13}. The tetrahedron method¹⁴ was used. From the band structure we calculated the optical conductivity directly.¹⁵ It is well known that GGA underestimates the band gap, and hence the optical conductivity shows the peaks displaced towards lower energies relative to actual experiments. However, the shapes and intensities are expected to be correct.

We notice the importance of including spin-orbit and so to perform full relativistic, non-collinear calculations^{16,17}. Significant spin-orbit splittings in the range 50 meV to 530 meV can be obtained in these crystals and can be measured using current spectroscopic techniques. Still, spin-orbit interaction is largely ignored in most of DFT calculations^{18–21}. In our case, even for light transition metals, such as Ti, we can have a spin-orbit splitting of the order of 40 meV, which can be easily measured. The trigonal prismatic (T) geometry does not have inversion symmetry, and has a considerable spin-orbit splitting, specially around the high symmetry point K. The octahedral symmetry (O) has inversion symmetry, and no spin-orbit splitting can be observed.

We first explore how the band nesting applies to a prototypical case of the 2D STMDC, namely, T-WS₂. Fig. 1 shows the band structure and the electronic density of states (DOS) of WS₂. We can see that at the K point of the electronic band structure of WS₂, where the transitions with smaller energy happens, there is a contribution to the DOS, as expected, but it is small when compared to the peaks due to the very flat bands near the conduction band minimum between the M and the Γ points (see point marked as G in Fig. 1), which is not a high symmetry point. Still, this is not sufficient to explain

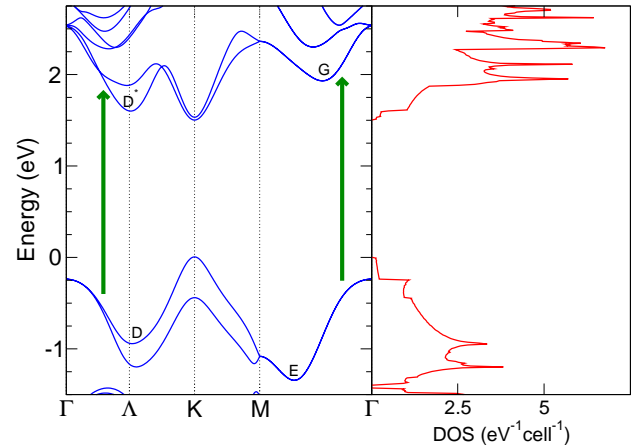


Figure 1. (Color online) The band structure, and the DOS of WS₂. The arrows indicate the transitions corresponding to the first peak in the optical conductivity. The letters E, G, D and D* are points with maximum, minimum or saddle points in the conduction or valence bands.

the high absorption peak that can be seen in the optical conductivity (see Fig. 2).

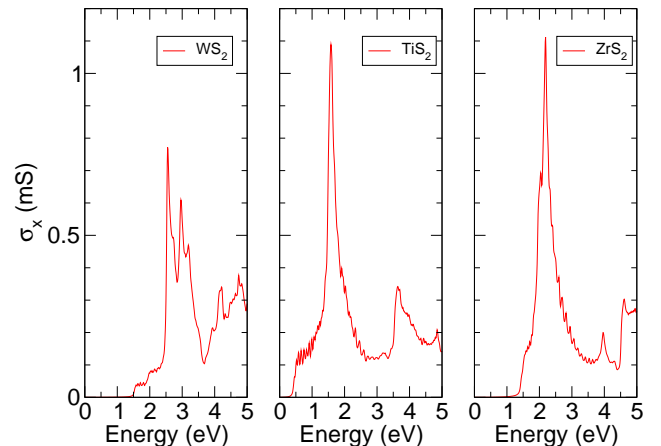


Figure 2. (Color online) Real part of the optical conductivity of WS₂, TiS₂, and ZrS₂ monolayers.

Since the important term is the gradient of the difference of energies between the conduction and valence band we plotted in Fig. 3 the difference in energy and the modulus of the gradient along the high symmetry path in the BZ.

The modulus of the gradient has small values for a large interval between the Γ and the Λ points (corresponding to transitions signaled in Fig. 1) which is the first large peak at 2.56 eV in the optical conductivity. It is also small near the right arrow of Fig. 1, at around 2.7 eV. Another extended line with low gradient is near the M point, in the direction of the Γ point. This is the origin of the peak in optical conductivity at 2.96 eV. Its

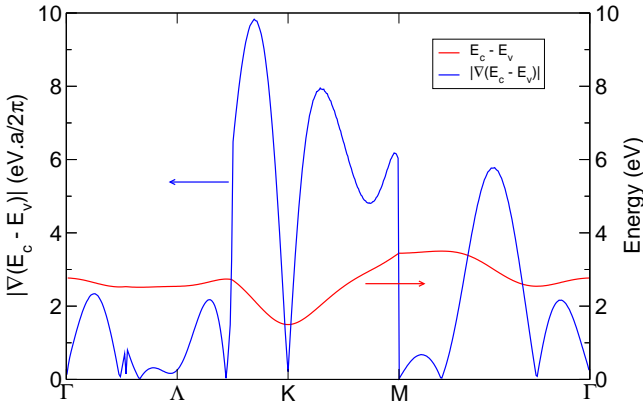


Figure 3. (Color online) Difference $E_c - E_v$ and modulus of its gradient, for WS₂ monolayer, in the high symmetry path. a is the lattice constant.

intensity is certainly helped by the degenerescence of the bands between M and Γ . We consider these extended regions where $|\nabla_k (E_c - E_v)| \ll 1 \text{ eV}/(2\pi/a)$ as *band nesting* ($2\pi/a$ is the modulus of the reciprocal lattice vector).

We have studied eleven compounds in the 2D STMDC family and found similar behavior including the ones with octahedral coordination. They have a different band structure from the trigonal prismatic polytype, and the question arises whether they will also show band nesting. Fig. 4 shows the band structure and DOS of another prototypical material: O-TiS₂ single layer. This material exists in the bulk with this coordination, and was predicted to be an energetically stable semi-metal¹⁸. However, our calculations show it to be an indirect band gap semiconductor, with a small gap. Experimentally, the bulk form of TiS₂ is a very narrow band gap semiconductor^{22,23} ($E_g \approx 0.3 \text{ eV}$). Since the DFT technique we use for these calculations is well known to underestimate the gap, we expect it to be even larger than what we obtain.

We first note that, since there is no spin-orbit splitting, all the bands shown are degenerate, which increases by a factor of two the density of states of this material. If we observe the energy gradients (Fig. 5), we notice that $|\nabla_k (E_c - E_v)| \ll 1 \text{ eV}/(2\pi/a)$ in the regions corresponding to the arrows of Fig. 4. The existence of another band below, and very near, the valence band prompted us to plot its gradient as well. Since it has transition energies very close to the ones from the highest occupied band, it mostly reinforces the peaks due to the band nesting. All the three transitions have similar energies, being the strongest near M at 1.5 eV; the others contribute to the large broadening of the peak in the optical conductivity (Fig. 2).

We explored all the BZ to find the extension of this band nesting. Figure 6 shows $|\nabla_k (E_c - E_v)|$ for TiS₂. In white we have the zone corresponding to values less than $1 \text{ eV}/(2\pi/a)$, which is the criteria we established. It can be seen that band nesting extends significantly beyond the high symmetry lines. The larger the area,

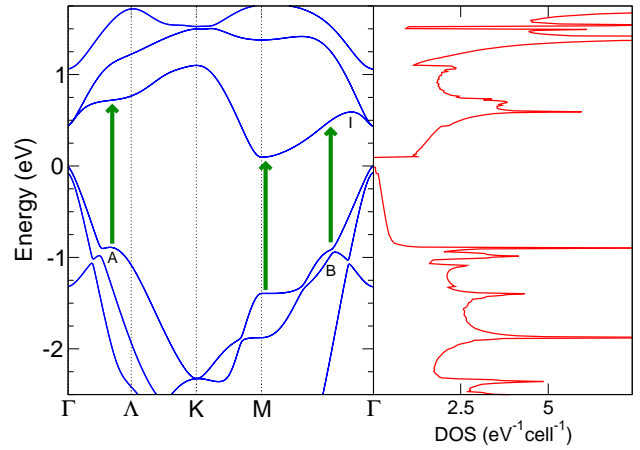


Figure 4. (Color online) Band structure and DOS of TiS₂ single layer. The arrows indicate the transitions corresponding to the large peak in the optical conductivity, with maximum at 1.58 eV. The letters A, B and I are points with maximum, minimum or saddle points in the conduction or valence bands.

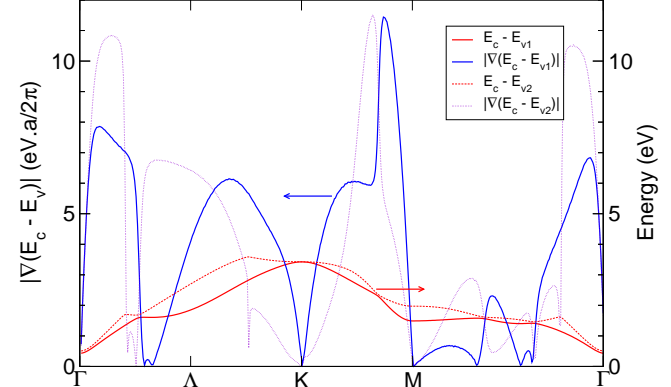


Figure 5. (Color online) Difference $E_c - E_v$ and modulus of its gradient, for TiS₂ monolayer, in the high symmetry path. E_{v1} indicates the highest occupied band, while E_{v2} indicates the second highest occupied band. a is the lattice constant.

the more intense the absorption peak is expected to be.

Another element of this family, ZrS₂, behaves in a similar way. ZrS₂ has the same octahedral structure and the same number of valence electrons as TiS₂. But in this case, the gap is much wider, as can be seen in Fig. 7.

The transitions marked by the arrows in Fig. 7 correspond to regions where the gradient of $E_c - E_v$ is small (Fig. 8). Hence, the absorption is very high at these energies, as can be seen in Fig. 2. There we have two very close peaks, forming a very broad peak. They correspond to a transition at the M point with an energy $E = 2.0 \text{ eV}$, and the transition indicated by the letter A with an energy $E = 2.2 \text{ eV}$. The transitions at B ($E = 1.88 \text{ eV}$) also give some contribution to the broadening of the peak in the optical conductivity. The transition at M is even stronger than for TiS₂. Both TiS₂ and ZrS₂ have ab-

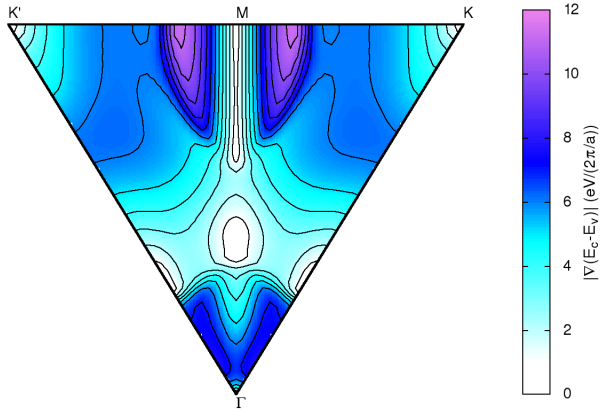


Figure 6. (Color online) Map on the BZ of $|\nabla_k (E_c - E_v)|$ for TiS_2 . a is the lattice constant.

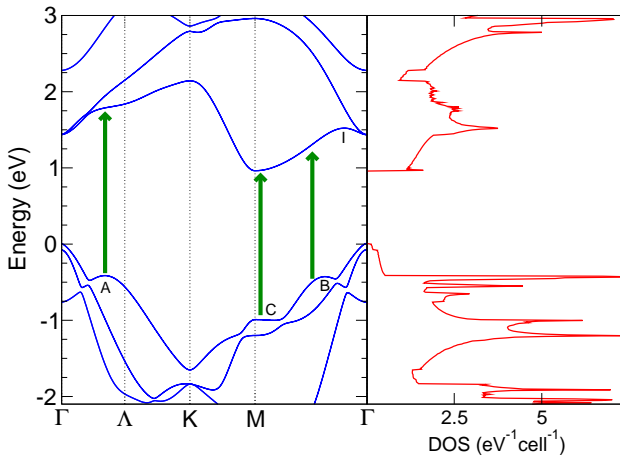


Figure 7. (Color online) Band structure and DOS of ZrS_2 single layer. The arrows indicate the transitions corresponding to the first peak in the optical conductivity. The letters A, B, C and I are points with maximum, minimum or saddle points in the conduction or valence bands.

sorption at lower energies than the corresponding to these transitions, but the intensity is almost an order of magnitude smaller. It is interesting to note that TiS_2 and ZrS_2 have a larger optical conductivity than the corresponding systems based on W or Mo.

We have verified all these results for all elements of the 2D STMDC that include WS_2 , WSe_2 , MoS_2 , MoSe_2 , in

the trigonal form, and TiS_2 , ZrS_2 , ZrSe_2 , PdS_2 , PdSe_2 , PtS_2 , PtSe_2 in the octahedral form and the band nesting is qualitatively the same. The only variation that we find is quantitative, namely, the intensity of the optical response changes from system to system. However, the presence of band nesting is ubiquitous in this family of 2D materials.

In conclusion, we have shown that 2D STMDC forms a class of materials with omnipresent band nesting. This feature of their band structure leads to a large optical response with peaks in the optical conductivity. This result indicates that even in 2D form, these materials present strong photon-electron coupling. Although, we have done the calculations in the linear response regime, it is clear that for the trigonal prismatic systems, that lack inversion symmetry, there will also be strong non-linear optical response allowing their use in photonics and opto-electronics. The existence of large electron-photon interaction in 2D opens up the possibility to exciting opportunities for basic research as well as for applications for 2D materials.

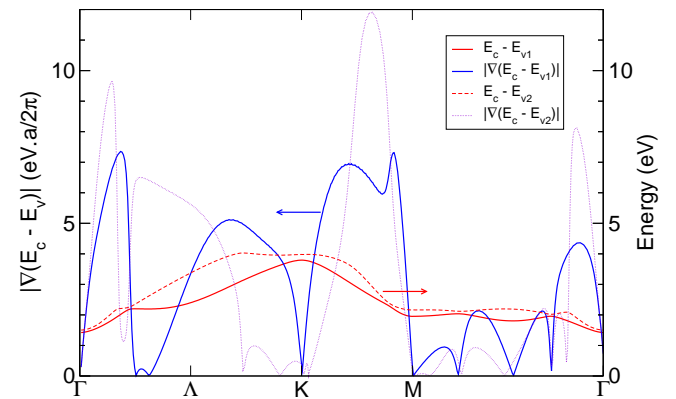


Figure 8. (Color online) Difference $E_c - E_v$ and modulus of its gradient, for ZrS_2 monolayer, in the high symmetry path. E_{v1} indicates the highest occupied band, while E_{v2} indicates the second highest occupied band. a is the lattice constant.

We gratefully acknowledge Jeil Jung Woo and the computer resources from TACC. RMR is thankful for the financial support by FEDER through the COMPETE Program and by the Portuguese Foundation for Science and Technology (FCT) in the framework of the Strategic Project PEST-C/FIS/UI607/2011 and grant nr. SFRH/BSAB/1249/2012. We acknowledge the NRF-CRP award "Novel 2D materials with tailored properties: beyond graphene" (R-144-000-295-281).

¹ J. Wilson, F. Di Salvo, and S. Mahajan, *Adv. Phys.* **24**, 117 (1975)

² Q. H. Wang *et al.*, *Nature Nanotechnology* **7**, 699 (2012)

³ M. Chhowalla *et al.*, *Nature Chemistry* **5**, 263 (2013)

⁴ M. S. Fuhrer and J. Hone, *Nature Nanotechnology* **8**, 146 (2013)

⁵ K. F. Mak *et al.*, Phys. Rev. Lett. **105**, 136805 (2010)

⁶ A. H. Castro Neto and K. Novoselov, Rep. Prog. Phys. **74**, 082501 (2011)

⁷ L. Britnell *et al.*, Science, 2 May 2013 (10.1126/science.1235547) (in press)

⁸ K. Gofron *et al.*, Phys. Rev. Lett. **73**, 3302 (1994)

⁹ P. Giannozzi *et al.*, J. Phys.-Cond. Matter **21**, 395502 (2009)

¹⁰ We used the pseudopotentials from the QUANTUM ESPRESSO distribution when available and if they passed the quality tests. Otherwise, we used pseudopotentials produced by us, subject to the same tests. The pseudopotentials were produced using the ATOMIC code by A. Dal Corso, that comes in the QUANTUM ESPRESSO distribution.

¹¹ J. P. Perdew, K. Burke, and M. Ernzerhof, Phys. Rev. Lett. **77**, 3865 (1996)

¹² H. J. Monkhorst and J. D. Pack, Phys. Rev. B **13**, 5188 (1976)

¹³ Single layer samples were modeled in a slab geometry by including a vacuum region of 45 Bohr in the direction perpendicular to the surface. A grid of $16 \times 16 \times 1$ \mathbf{k} -points was used to sample the BZ. The energy cutoff was 50 Ry. The atomic positions were optimized using the Broyden-Fletcher-Goldfarb-Shanno (BFGS) method for the sym-

metric structure. The lattice parameter a was determined by minimization of the total energy. The electronic density of states was calculated by sampling $48 \times 48 \times 1$ points of the BZ, and broadened with a 0.01 eV Gaussian width. A Gaussian broadening of 0.05 eV width was applied in the optical conductivity.

¹⁴ P. E. Blochl, O. Jepsen, and O. K. Andersen, Phys. Rev. B **49**, 16223 (1994)

¹⁵ The dielectric permittivity and the optical conductivity were calculated using a modified version of the EPSILON program of the QUANTUM ESPRESSO distribution, to account for full relativistic calculations.

¹⁶ Z. Y. Zhu, Y. C. Cheng, and U. Schwingenschlögl, Phys. Rev. B **84**, 113201 (2011)

¹⁷ A. Ramasubramaniam, D. Naveh, and E. Towe, Phys. Rev. B **84**, 205325 (2011)

¹⁸ C. Ataca, H. Şahin, and S. Ciraci, J. Phys. Chem. C **116**, 8983 (2012)

¹⁹ S. Bhattacharyya and A. K. Singh, Phys. Rev. B **86**, 075454 (2012)

²⁰ Y. Ding *et al.*, Physica B: Condensed Matter **406**, 2254 (2011)

²¹ A. Kuc, N. Zibouche, and T. Heine, Phys. Rev. B **83**, 245213 (2011)

²² C. A. Kukkonen *et al.*, Phys. Rev. B **24**, 1691 (1981)

²³ C. H. Chen *et al.*, Phys. Rev. B **21**, 615 (1980)